ISSN 2250-3153

A New Impulse Noise Detection and Filtering Algorithm

Geeta Hanji, M.V.Latte

Abstract- A new impulse detection and filtering algorithm is proposed for restoration of images that are highly corrupted by impulse noise. It is based on the average absolute value of four convolutions obtained by one-dimensional Laplacian operators. The proposed algorithm can effectively remove the impulse noise with a wide range of noise density and produce better results in terms of the qualitative and quantitative measures of the images even at noise density as high as 90%. Extensive simulations show that the proposed algorithm provides better performance than many of the existing switching median filters in terms of noise suppression and detail preservation.

Index Terms- image processing, impulse noise, noise suppression, detail preservation

I. INTRODUCTION

During image acquisition or transmission, digital images could be contaminated by impulse noise. Two common types of impulses are the salt-and-pepper noise and the random-valued noise [1, 2]. For image corrupted by salt-and-pepper impulse noise, the noisy pixels can take only the maximum and the minimum value in the dynamic range. For 8-bit pixel, the maximum value is 255 and the minimum value is 0. In the literature, a large number of algorithms have been proposed to remove impulse noise while preserving image details [1–9]. One of the most popular and robust nonlinear filter is the standard median filter (SMF) [1], which exploits the rank-order information of pixel intensities within a filtering window and replaces the center pixel with the median value. Conventional median filtering approaches apply the median operation to each pixel without considering whether it is uncorrupted or corrupted, thus the impulse noise is removed at the expense of blurred and distorted features. Improved filtering algorithms employ an impulse-noise detector to determine which pixels should be filtered, hence only those pixels identified as "corrupted" would undergo the filtering process, while those identified as "uncorrupted" would remain intact. The adaptive median filter (AMF) [2] ensures that most of the impulse noise can be detected even at a high noise level provided that the window size is large enough. But, it increased the computation complexity especially at high density impulse noise. The convolution-based impulse detector and switching median filter (CD-SMF) algorithm [3] distinguishes whether the interest pixel is noise or not depending on a threshold determined by computer simulations. [4] processes the corrupted image by first detecting the impulse noise and uses a fixed 3×3 window size to handle the corrupted pixel for removal of impulse noises. It is found that CD-SMF and A new Impulse Detection and Filtering method for removal of Wide Range Impulse Noises, IDFRWRIN[5] ,will exhibit serious image blurring for high density impulse noise [3, 5, 6]. In this paper, we propose new impulse noise detection and filtering algorithm that can effectively remove a wide range impulse noise while preserving image details. The proposed algorithm is shown to achieve excellent performance across a wide range of noise densities varying from 10% to 90%. The organization of the rest of this paper is as follows. In the next section, new impulse noise detection and filtering algorithm is described in detail. In Section 3, some experimental results are presented with discussion. The concluding remarks are given in Section 4.

II. THE PROPOSED IMPULSE NOISE DETECTION AND FILTERING ALGORITHM

In this paper, noise is assumed to be salt and pepper impulse noise. Pixels are randomly corrupted by two fixed extreme values, 0 and 255 (for 8-bit monochrome images) generated with the same probability [6]. There are three steps (steps (a)–(c)) in our proposed algorithm for impulse detection and filtering. After classifying corrupted and uncorrupted pixels (see steps (a) and (b)), we replace the corrupted pixel by the suitable value of the sorted sequence of its neighborhood values (see step(c)). We repeat steps (a)–(c) for S iterations to get the convergent recovery image.

Step (a): The input image Xij is first convolved with a set of convolution kernels. Here, four one-dimension Laplacian operators shown in Fig. 1 are used, each of which is sensitive to edges in a different orientation [3]. Then, the average absolute value of these four convolutions (denoted as r_{ij}) is used for impulse detection, which can be represented as:

$$r_{ij} = \mathrm{Avg}\left\{\left|X_{ij} \otimes K_t\right| \,\middle|\, t = 1, 2, 3, 4\right\} \quad (1)$$

where K_t is the t_{th} kernel and $\otimes$ denotes a convolution operation. We compare r_{ij} with a threshold T to determine whether a pixel is corrupted,

$$\alpha_{ij} = \begin{cases} 1, & r_{ij} > T \\ 0, & r_{ij} \leqslant T \end{cases} \quad (2)$$

If $\alpha_{ij}=1$, then the pixel Xij is marked as noise candidate; otherwise the pixel Xij is noise-free. A reasonable threshold T can be determined as follows: Consider an example of a 3×3 window (i.e., W =3 X 3), in which four thresholds μ_k , k = 0, 1, 2, 3, are needed. The median of the absolute deviations from the median (MAD), MAD=median $\{|x_{i-s,\ j-t} - x_{i,j}| \mid (s,t) \in W\}$ is a robust estimate of dispersion [12].

Specifically the thresholds are described as

$T = s \cdot MAD + \mu_k;\ 0 \leq k \leq 3$ (3)

$[\ \mu_0, \mu_1, \mu_2, \mu_3\ ] = [40, 25, 10, 5\ ]$ (4)

Here parameter s (> 0) varies for different images degraded with different noise ratios, & is also observed empirically that good results could be obtained using $0 \leq s \leq 0.6$, in suppressing impulse noise for various images. Hence due to the robustness of

the algorithm, the determination of the thresholds is simplified to the adjustment of parameter s.

Step (b): If the interesting pixel Xij is marked as noise candidate, we use a fixed 3×3 window W shown in (2) for further processing:

$$W = \begin{bmatrix} a_0 & a_5 & a_3 \\ a_6 & a_1 & a_7 \\ a_4 & a_8 & a_2 \end{bmatrix} = \begin{bmatrix} X_{i-1,j-1} & X_{ij-1} & X_{i,j+1} \\ X_{i-1,j} & X_{ij} & X_{i+1,j} \\ X_{i-1,j+1} & X_{ij+1} & X_{i+1,j+1} \end{bmatrix}$$

By sorting all the elements a0, a1, a2, a3, a4,a5,a6,a7 and a8 in ascending order, we get a sorted sequence: b0, b1, b2, b3, b4,b5,b6,b7 & b8, where b0 <b1 < b2 < b3 < b4 < b5 < b6 <b7 < b8. If Xij satisfies the following cases, the pixel will be considered a noise-free pixel and retain its value:

Case 1: $a_0 < Xij < a_8$

Case 2: $Xij = b_8 \neq 255$

Case 3: $Xij = b_0 \neq 0$

1. Case 1 indicates that Xij is not an extreme value.
2. Case 2 indicates that Xij is not a salt impulse noise.
3. Case 3 indicates that Xij is not a pepper impulse noise.
4. If Xij does not satisfy Cases 1–3, the pixel will be regarded as a noisy pixel.

So, Xij is replaced by the mean of noise free pixels.

III. EXPERIMENTAL RESULTS

In this experiment, The performance is tested with different gray scale images such as Lena, Girl, and Baboon with size 256×256. In the simulation, images are corrupted by "salt" (with value 255) and "pepper" (with value 0) noise with equal probability. The noise levels are widely varied from 10% to 90% with increments of 10%, and the restoration performance are quantitatively measured in terns of PSNR in dB and computation time in seconds. A comparison of these performance measures with various algorithms including SMF, AMF, CD-SMF and A new Impulse Detection and Filtering method for Removal of Wide Range Impulse Noises (IDFRWRIN) [4] are presented in Tables 1–2. It is observed that the proposed algorithm can provide better performance in terms of image quality and computation time. For every noise level, our algorithm achieves better PSNR than SMF, AMF, CD-SMF and & IDFRWRIN. Though the computation time of SMF and AMF is shorter than our algorithm, but their PSNR performance is not good. Extensive simulations show that our algorithm converges with S = 2 iteration for noise density below 30%, with S=4 iterations for noise density from 40% to 70%, and with S = 5 iterations for density higher than 80%. Fig. 1 shows the original test images. Figs. 2–3 show the subjective visual qualities of the filtered images using various algorithms for the image "Lena" corrupted by 50% and 80% impulse noise. It can be seen that for different noise density the SMF suppress the impulses but introduce the obvious blur effect. Our algorithm can achieve better PSNR visual quality while preserving image detail very well for a wide range of noise density. Figs. 4 and 5 show the restoration results for the Girl image corrupted by 50% & 80% noise, respectively. These results also reveal that the. proposed algorithm exhibits better visual quality.

IV. CONCLUSION

In this paper, a new algorithm for impulse detection and filtering is proposed. The proposed algorithm can not only achieve better image quality, but also have shorter computation time. Extensive simulations reveal that the proposed algorithm provides better performance than many of the existing switching median filters in terms of noise suppression and detail preservation. The proposed algorithm shows stable performance across a wide range of noise densities varying from 10% to 90%, and is suitable for real-time implementation since it uses a fixed 3×3 window for filtering processing.

Figure1. The original image Lena and Girl

Figure 2. Image restoration results: (a) Lena image corrupted with 50% impulse noise (b) SMF (c) AMF (d) CD-SMF (e) IDFRWRIN (f) Proposed

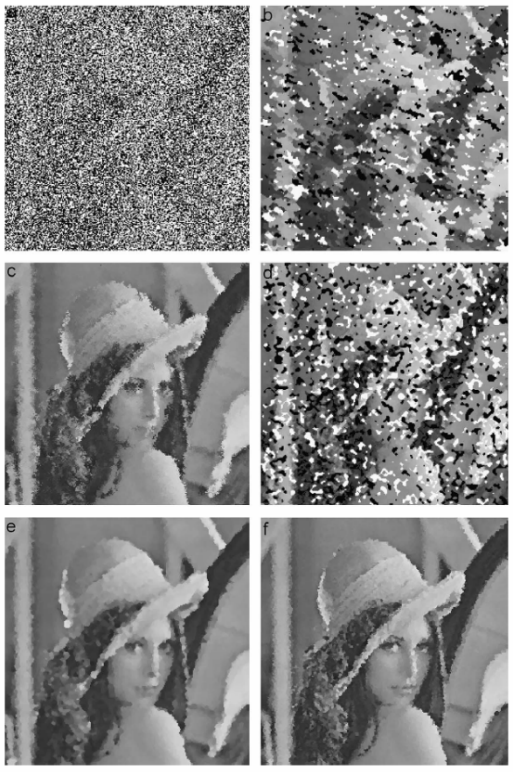

Figure 3.Image restoration results:(a)Lena image corrupted with 80% impulse noise(b) SMF(c) AMF (d) CD-SMF (e)IDFRWRIN (f) Proposed

TABLE (1): PSNR (DB) AND COMPUTATION TIME (SEC) FOR VARIOUS ALGORITHMS FOR LENA IMAGE

NOISE DENSITY	ALGORITHM									
	SMF		AMF		CD-SMF		IDFRWRIN		PROPOSED	
	PSNR	TIME	PSNR	TIME	PSNR	TIME	PSNR	TIME	PSNR	TIME
10%	29.93	0.61	35.57	0.639	32.94	0.938	39.09	0.764	40.2	0.762
20%	28.36	0.625	32.94	0.639	30.97	0.823	34.32	0.734	36.32	0.732
30%	26.42	0.625	30.72	0.639	29.62	0.823	32	0.734	33.4	0.721
40%	23.99	0.625	28.94	0.657	27.83	0.828	30.27	0.734	32.27	0.714
50%	21.7	0.625	27.37	0.671	26	0.938	28.54	0.735	30.54	0.714
60%	19.47	0.64	26.17	0.718	22.55	0.796	27.33	0.75	29.63	0.71
70%	15.98	0.609	24.18	0.859	17.39	0.843	26	0.765	28	0.735
80%	13.04	0.609	22.39	1.531	12.37	0.86	24.53	0.764	26.53	0.734
90%	8.94	0.609	20.17	10.6	8.46	0.764	22.2	0.765	24.2	0.745

TABLE 2: PSNR (DB) AND COMPUTATION TIME (SEC) FOR VARIOUS ALGORITHMS FOR GIRL IMAGE

NOISE DENSITY	ALGORITHM

	SMF		AMF		CD-SMF		IDFRWRIN		PROPOSED	
	PSNR	TIME	PSNR	TIME	PSNR	TIME	PSNR	TIME	PSNR	TIME
10%	31.89	0.609	37.33	0.639	35.34	0.823	42.11	0.735	44.12	0.713
20%	31.05	0.65	35.57	0.656	33.07	0.86	37.33	0.734	39.03	0.714
30%	28.73	0.61	33.65	0.640	31.14	0.938	34.90	0.75	36.12	0.72
40%	26.73	0.69	31.79	0.656	29.20	0.86	32.80	0.75	34.71	0.714
50%	23.98	0.625	30.34	0.688	27.26	0.823	32.81	0.75	34.86	0.723
60%	20.32	0.609	28.49	0.75	22.95	0.823	31.50	0.75	33.25	0.723
70%	16.67	0.625	27.02	0.875	16.05	0.836	29.80	0.75	31.81	0.723
80%	12.66	0.625	24.57	3.03	11.52	0.796	28.73	0.75	30.45	0.723
90%	8.29	0.610	23.12	11.2	7.34	0.836	29.84	0.74	31.65	0.72

REFERENCES

[1] J. Wang, "Fundamentals of erbium-doped fiber amplifiers arrays (Periodical style—Submitted for publication)," *IEEE J. Quantum Electron.*, submitted for publication.

[2] Wakeham.K.J. "Introduction to chassis design revision 1.0" Undergraduate diss., Memorial University of Newfoundland and Labrador. 2009

[3] Beleandez, T. Neipp, C. And Belea, N.A, "Numerical and experimental analysis of a cantilever beam: A laboratory project to introduce geometric Nonlinearity in mechanics of materials". International journal of engng. Ed. vol.19 No 6 pp 885-892. 2003

[4] Karaoglu, C. and Kuralay, N.S., "Stress analysis of truck chassis with riveted joints", Elsevier science Publishers B.V Amsterdam, the Netherlands Vol.38 pp 1115-1130. 2000

[5] Ye.N and Moan T 2007, "Static and Fatigue analysis of three types of Aluminum Box-Stiffener/web Frame connections, International Journal of Fatigue 29 pp1426- 1433

[6] Crouse W.H and Anglin D.L, Automotive Mechanics, Tata McGraw Hill Education Pvt.Ltd. pp. 658-711 2007

[7] National Code of Practice, Heavy Vehicle Modifications Section H Chassis Frame.

[8] National Code of Practice, Heavy Vehicle Modifications Section J Body Mounting.

[9] Meiyalagan, M Anbarasu, M and Dr.Sukumar.S, "Investigation on cold formed C Section Long Column with Intermediate Stiffener and corner lips under axial compression" International Journal of applied engineering research, Dindigul, Vol.No.1 pp 28-41. 2010

[10] Young B, "Tests and design of fixed ended cold formed steel plain angle columns, Journal of structural engineering © ASCE / 19311940, 2004

[11] Martin H.Sadd (2004), "Elasticity Theory, Applications and Numerics" Elsevier, a division of Reed Elsevier India Private Limited.

[12] Timoshenko S and Goodier J.N, "Theory of Elasticity" Mc-Graw Hill Book Company, Inc.

[13] Reimpell J., Stoll H., Betzler J.W., "The Automotive chassis: Engineering Principles" Second Edition. Butterworth Heinemann, A division of Reed Educational and Professional Publishing Ltd.

First Author – Geeta Hanji, [1]ECE Department, P.D.A.Engg. College, Gulbarga,Karnataka, India & Research Scholar (Part-Time), J.N.T.University,Hyderabad,India. Email: geetanjalipatil123@gmail.com

Second Author – M.V.Latte, ECE Department, J.S.S.Mahavidyapeetha, Bangalore, Karnataka, India, Email: mvlatte@rediffmail.com